**NURETH14-469** 

# A MODEL FOR DROPLET ENTRAINEMENT RATE IN HORIZONTAL STRATIFIED FLOW

F. Henry <sup>1</sup>, M. Valette <sup>2</sup> and Y. Bartosiewicz <sup>1</sup>

I Université catholique de Louvain (UCL)
 Institute of Mechanics, Materials and Civil Engineering (iMMC)
 Bat. Stévin, Place du Levant 2
 B-1348 Louvain-la-Neuve, Belgium

<sup>2</sup>Commissariat à l'Energie Atomique et aux énergies renouvelable (CEA), DEN/DER/SSTH 17, Avenue des Martyrs, 38000 Grenoble, France

#### **Abstract**

This work proposes an original approach for modeling the entrainment of droplets in a horizontal stratified two-phase wavy flows. This mechanistic model is based on the ripple-waves breakout and entrainment phenomenon by estimating the liquid mass pulled off the wave crests during their fragmentation. The paper presents the modeling procedure for estimating the wavelength of these ripples and the related entrained liquid volume. In regards to these parameters, it is shown that a relatively simple methodology can be obtained to ease the implementation in a system code. This work aims at substituting the current existing empirical correlations in the system code CATHARE 3 by using a flowfield for a liquid dispersed phase.

## Introduction

Nuclear safety studies are conducted by analyzing the impact of several hypothetical accidents on the behavior of the nuclear reactor. For reactors of PWR type, one major accident to consider is the so-called Loss Of Coolant Accident (LOCA). Part of the water leaves the reactor coolant system through a rupture in one pipe. The blowdown at the break, which results of the rupture, involves an emptying of the circuit and hence a depletion in core cooling. The discharge of the circuit leads to the emergence of many local transient phenomena that give rise to a depressurization of the core. The loss of pressure causes primary water boiling in the core, such that a vapour-liquid flow appears in the downcomer, the hot legs and the steam generators. Security systems come into action and the core reflooding begins. This step is strongly affected by the evolution of the pressure in the primary circuit which affects the water level balance in the core. One of the phenomena that affects these variations is the vaporization of entrained droplets in the steam generator. Therefore, the knowledge of the quantity and the characteristics of entrained droplets is crucial in the core reflooding process analysis.

Among the flows that takes place during the core reflooding process, a wavy stratified flow may

occur in the hot leg. Interfacial shear forces involve the emergence, development and fragmentation of waves resulting in the apparition of dispersed liquid droplets in the gas phase. Those droplets are transported by the steam towards the steam generator and may eventually deposit along their path. As a consequence, the dynamics of entrainment and deposition of droplets from this wavy stratified flow triggers the amount of liquid which could reach the steam generator. Therefore determining the characteristics and quantities of droplets which are entrained from the liquid phase in a wavy stratified flow is of interest for calculating the necessary reflooding time.

The current nuclear safety system code of the CEA, called CATHARE, uses a two field approach to model the flow in a nuclear reactor. Thus it is not able to directly model a dispersed phase in a stratified flow. However the new version in development allows the use of a three field model which is the most appropriate approach to tackle such phenomena. This study presents a preliminary approach to add a source term which mimics the mass exchange between the continuous liquid and the droplet fields for a one-dimensional pipe.

The mass balance equations for the continuous liquid (lc) and the dispersed liquid (ld) phases are the following:

$$\frac{\partial}{\partial t} (A \alpha_{lc} < \rho_{lc} >) + \frac{\partial}{\partial z} (A \alpha_{lc} < \rho_{lc} u_{lc} >) = +A (\Gamma_d - \Gamma_e) + A \Gamma_{lc,v} 
\frac{\partial}{\partial t} (A \alpha_{ld} < \rho_{ld} >) + \frac{\partial}{\partial z} (A \alpha_{ld} < \rho_{ld} u_{ld} >) = -A (\Gamma_d - \Gamma_e) + A \Gamma_{ld,v}$$
(1)

where  $\Gamma_d$  is the deposition rate (the amount of liquid deposed on the liquid film by units of time and surface),  $\Gamma_e$  the entrainment rate and  $\Gamma_{k,v}$  the amount of the liquid phase k vaporized by unit of time and surface.

Thus the study presented here describes a method for the determination of this mass exchange term  $\Gamma_e$  which represents the mass of liquid pulled off the continuous liquid phase as droplets into the vapor phase by unit of time and surface.

#### 1 A brief review of entrainment models

The modeling of the droplet entrainment phenomenon in horizontal pipe for stratified flows has not been as developed as its counterpart for vertical/annular flows. However few correlations are proposed in the open literature, like the pioneering work of Hutchinson and Whalley [1], and more recent works of Hewitt and Govan [2] or Williams and Hanratty [3]. Those models are all strongly dependent on dimensionless groups, based on their based experimental conditions and have little or no dependence on the physical processes which lead to waves fragmentation and droplet entrainment.

Moreover, most of those models are introduced for fully-developped flows in horizontal pipe. They are based on an equilibrium assumption [4, 3] which postulates that entrainment rate is equal to the deposition rate. Therefore, they are questionable for non-fully-developed flows occuring in the hot leg of a PWR; this assumption is indeed not suited for transient two-phase flows in mechanical non-equilibrium.

As those models are essentially semi-empirical, their predictions are questionable far from their based experimental conditions. Regrettably those experimental apparatus have dimensions (i.e. diameter) much smaller than real pipe dimensions of a NPP.

Furthermore, the term for droplet entrainment rate in stratified flows in the current version of CATHARE 3 is based on the correlation of Hewitt and Govan [2] which has been originally

developed for vertical flows.

The questionability of the current models in the open literature upon their abilities to predict the droplet entrainment in transient two-phase stratified flows in horizontal pipes of large diameters led to this new model. The early idea was to develop a model based as far as possible on a mechanistic approach.

#### 2 The entrainement model

## 2.1 Mechanics of droplet entrainment

In 1969, Woodmansee and Hanratty [5] realized important experiments showing that interfacial instabilities development have a clear impact on entrainment phenomena. They observed that droplets came by the acceleration, lifting and subsequent shattering of ripples waves present on primary waves having a much larger wavelength called liquid roll-up structures. As the wavelength of those ripples waves is strongly smaller than that of primary waves, the droplet entrainment is caused by many ripples which are swept-off of each roll-wave. Also, the observed lifetime of those ripples was much shorter than that of the primary structures. Therefore, the entrainment of droplets could be attributed to the development of this secondary instability which is essentially a Kelvin-Helmholtz instability [5]. The model described below aims at taking into account this physical process to predict the droplet entrainment rate. The general approach is based on the work of Holowach and al. [6] for vertical annular flows but it was largely modified to suit the horizontal stratified flow configuration.

## 2.2 Model overview

An analysis on a control volume in a wavy stratified horizontal flow is made in order to find out an expression for the droplet entrainment rate. Based on the Woodmansee and Hanratty [5] description for waves breakup, the amount of liquid entrained as droplets in the dispersed liquid phase is equal to the amount of liquid pulled up at the crest of ripple waves multiplied by the number of those waves. Obviously this number is calculated based on the assumption that all the ripple waves in the control volume have the same critical wavelength. This assumption implies that from all possible wavelengths the only wave that develops will be that corresponding to the rate of the largest amplification. In order to get the dimension of an entrainment rate  $[kg \, m^{-2} \, s^{-1}]$ , the model must take into account the characteristic time of the phenomenon and the interfacial gas-liquid area (Equ. 2):

$$\Gamma_e = \frac{\rho_l \, V_{entr,rw} \, N_{rw,f}}{A_{cv} \, \tau_{c,e}} \tag{2}$$

where  $\rho_l V_{entr,rw}$  is the amount of liquid pulled up at the crest of a ripple wave (rw),  $N_{rw,f}$  the number of ripple waves ripped off,  $A_{cv}$  the interfacial area of the control volume and  $\tau_{c,e}$  the characteristic time of the entrainment phenomenon.

## 2.3 Parameters Description

The entrained volume at a fragmented wave crest is function of the ripple waves geometry and so, as the ripple waves are assumed to have **three-dimensional sine geometry**, the volume depends on the ripples wavelength. In reality, the wave geometry differs from sine and has a more truncated geometry on one end. Nevertheless the sine wave is a reasonable approximation

for the modeling of the waves development and fragmentation.

The control volume dimension is assumed to be the cross section area of the pipe multiplied by the wavelength of the roll-up structures. Moreover, the interfacial area is equal to the chord of the wavy pattern in the transverse direction multiplied by the roll waves wavelength. As the interfacial area is wavy, a geometric parameter  $\beta_{cv}$  is added to take into account the curvature of the interfacial surface:

$$A_{cv} = l_i \times \lambda_q \times \beta_{cv} \tag{3}$$

where  $l_i$  is the width (chord) of the interface in the cross-section plane,  $\lambda_g$  the wavelength roll waves in the axial direction,  $\beta_{cv}$  the geometrical parameter. The number of ripple waves (Equ. 4) which is fragmented is proportional to the total number of ripple waves in the control volumes:

$$N_{rw,f} = \frac{N_{rw,f}}{N_{rw,tot}} N_{rw,tot} = f_{rw} \frac{\lambda_g}{\lambda_{rw}} \frac{l_i}{\lambda_{rw}}$$
(4)

where  $N_{rw,tot}$  is the total number of ripple waves in the control volume,  $\lambda_{rw}$  the wavelength of ripples and  $f_{rw}$  the proportion of fragmented ripples waves.

A simple expression (Equ. 5) is finally obtained for the entrainment rate in horizontal pipes:

$$\Gamma_e = \rho_l \frac{V_{entr,rw} f_{rw}}{\beta_{cv} \lambda_{rw}^2 \tau_{c,e}} \tag{5}$$

This model requires the knowledge of the critical wavelength of the ripples  $\lambda_{rw}$ , the entrained volume  $V_{entr,rw}$  and the characteristic time  $\tau_{c,e}$ .

This formulation is independent of the control volume; in terms of implementation in CATHARE, the control volume is dictated by the choice of the one-dimensional mesh. It is assumed that CATHARE will be able to capture and transport large wavelengths such as the roll-waves coming from upstream perturbations. Therefore, if the wavelength of the ripple waves is known, the total number of ripples in a control volume could be easily determined. The coefficient  $f_{rw}$  could be then evaluated providing a criteria for the fragmentation of these ripples, based on a force balance and eventually on their relative location to the crest of a primary structure. In a first approach we could assume that all the ripples are fragmented and hence  $f_{rw} = 1$ . The coefficient  $\beta_{cv}$  is a correction coefficient taking into account the average curvature of the interface and the presence of a wavy pattern in the transverse direction; this coefficient could be evaluated analytically knowing the height of liquid and the wavy pattern.

The following sections are devoted to find expressions for  $\lambda_{rw}$  (Equ. 24) and  $V_{entr,rw}$ . Discussions about the choice of the entrainment characteristic time scale  $\tau_{c,e}$  is not the scope of this paper; even though a simple expression such as the ratio between the ripples wavelength and the relative gas velocity over the liquid could be found in [6], others formulations are possibles.

# 3 Critical wavelength

The sub-model concerning the evaluation of the critical wavelength of ripples waves is achieved by formulating a two-dimension linear stability analysis of the flow depicted Fig. 1. This work relies on earlier works about linear stability analysis conducted by de Crécy [7] or Barnea and Taitel [8]. Kelvin-Helmholtz linear stability has been used frequently in the past for determining whether a stratified flow is stable or unstable through the determination of a stability criterion. The classical inviscid Kelvin-Helmholtz instability analysis has been extended by Lin and Hanratty [9, 10], Barnea [11], and Barnea and Taitel [8] to viscous flows using one-dimensional averaged two-fluid models.

This analysis performed here is in the frame of the **viscous two-fluid model**. The stability of the interface between the gas and the liquid is studied on the basis of a small perturbation analysis assuming that the interface slope is small. This assumption allows the linearization of the fluid motion equations. The effect of viscosity is taken into account through closure laws for walls and interfacial friction factors. The originality of the study presented here comes from the choice of closure laws and the modeling of the pressure distribution in the pipe. As shown by Barnea and Taitel [11], the use of a constant pressure in the cross section is not acceptable for this case. Therefore the pressure repartition is assumed to be hydrostatic according:

$$\langle p_k \rangle = P_{i,k} + \rho_k g_\perp (h_i - h_{cq,k}) \tag{6}$$

where  $h_{cg,k}$  is the height of the center of phase k,  $h_i$  the height of the interface,  $P_{i,k}$  the pressure at the interface along the side of phase k and k, the space average pressure of phase k. The pressure jump through the interface is then evaluated with the Laplace's law:

$$P_{i,g} - P_{i,l} = \frac{\sigma}{R} = \sigma \frac{\delta^2 h_i}{\delta z^2} \tag{7}$$

where  $\sigma$  is the surface tension and 1/R = K is the surface curvature.

The purpose of the stability analysis is to find out the most amplified wavelength for a set of flow conditions (superficial velocities, pipe diameter, fluid characteristics,...). It is assumed that while this set remains constant the wavelength does not evolve during the wave development. Thereby, since the entrainment and deposition phenomena are supposed not influencing the growing wave shape, **no mass transfer** between the two phases is considered as a basic assumption of the stability analysis. Furthermore, the following assumptions are also used during the calculation procedure:

- No heat transfer between the two phases
- Both gas and liquid are incompressible

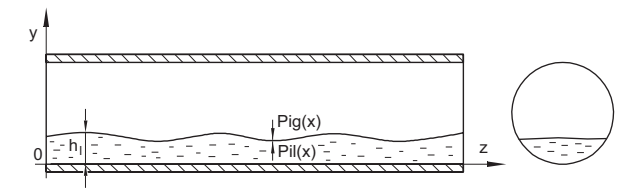


Figure 1: Schematic representation of horizontal two-phase stratified flow

The one-dimensional two-fluid model is based on cross-section averaging of the governing equations for each phase as follows. The continuity equations for the liquid and the gas are:

$$\frac{\partial}{\partial t} (\alpha_l \rho_l) + \frac{\partial}{\partial z} (\alpha_l \rho_l u_l) = 0$$

$$\frac{\partial}{\partial t} (\alpha_g \rho_g) + \frac{\partial}{\partial z} (\alpha_g \rho_g u_g) = 0$$
(8)

The momentum equations for each phase are:

$$\frac{\partial}{\partial t} (A_l \rho_l u_l) + \frac{\partial}{\partial z} (A_l \rho_l u_l^2) + A_l \frac{\partial}{\partial z} \langle p_l \rangle = A F_{fr,l} + A F_{fr,i,l} 
\frac{\partial}{\partial t} (A_g \rho_g u_g) + \frac{\partial}{\partial z} (A_g \rho_g u_g^2) + A_g \frac{\partial}{\partial z} \langle p_g \rangle = A F_{fr,g} + A F_{fr,i,g}$$
(9)

where A is the cross-section area and  $F_{fr}$  the friction forces at walls and at the interface. Obviously  $F_{fr,i,g} = -F_{fr,i,l}$ .

A small perturbation is then applied to the different variables: the velocities  $u_k$ , the volume fractions  $\alpha_k$  and thus the levels of the phases and interface in the pipe  $h_k$ , where the symbol denotes the steady-state value and the ' stands for the perturbation:

$$u_l = \bar{u}_l + u'_l \quad u_q = \bar{u}_q + u'_q \quad h_i = \bar{h}_i + h'_i \quad \alpha_l = \bar{\alpha}_l + \alpha'_l$$
 (10)

After some transformations and by substituting in the conservation equations the parameters according Equ. 10, the linearized form of the mass conservation equations (Equ. 11) and a combined linearized momentum equation (Equ. 12) can be obtained:

$$\frac{\partial u_g'}{\partial z} - \left[ \frac{\partial h_l'}{\partial t} + \bar{u}_g \frac{\partial h_l'}{\partial z} \right] \frac{1}{\bar{\alpha}_g} \frac{\partial \alpha_l}{\partial h_l} = 0$$

$$\frac{\partial u_l'}{\partial z} + \left[ \frac{\partial h_l'}{\partial t} + \bar{u}_l \frac{\partial h_l'}{\partial z} \right] \frac{1}{\bar{\alpha}_l} \frac{\partial \alpha_l}{\partial h_l} = 0$$
(11)

$$\rho_{l} \frac{\partial u'_{l}}{\partial t} + \rho_{l} \bar{u}_{l} \frac{\partial u'_{l}}{\partial z} - \rho_{g} \frac{\partial u'_{g}}{\partial t} - \rho_{g} \bar{u}_{g} \frac{\partial u'_{g}}{\partial z} + (\rho_{l} - \rho_{g}) g \frac{\partial h'_{i}}{\partial z} - \sigma \frac{\partial^{3} h'_{i}}{\partial z^{3}} - \left(\rho_{l} \frac{dh_{g,l}^{-}}{dh_{i}} - \rho_{g} \frac{dh_{g,g}^{-}}{dh_{i}}\right) g \frac{\partial h'_{i}}{\partial z} = F = -\frac{\tau'_{l}}{\alpha_{l}} \frac{S_{l}}{A} + \frac{\tau'_{i}}{\alpha_{l}} \frac{S_{i}}{A} + \frac{\tau'_{g}}{\alpha_{g}} \frac{S_{g}}{A} + \frac{\tau'_{i}}{\alpha_{g}} \frac{S_{i}}{A}$$

$$(12)$$

where F represents the friction terms at solid surfaces and at the interface for both phases. Differentiating Equ. 12 with respect to z and substituting Equ. 11 yields a single equation (Equ. 13) for the perturbed variable  $h'_i$ . The reasons to derive an equation based on the liquid height instead of the liquid volumetric fraction are practical: indeed this is the height at the center of the pipe which would be directly measured in an experiment and not an averaged void fraction.

$$\left[\frac{\partial^{2}h'_{i}}{\partial t^{2}}\right]\left[\frac{\rho_{l}}{\bar{\alpha}_{l}} + \frac{\rho_{g}}{\bar{\alpha}_{g}}\right] + \left[\frac{\partial^{2}h'_{i}}{\partial z\partial t}\right]\left[2\frac{\rho_{l}}{\bar{\alpha}_{l}}\bar{u}_{l} + 2\frac{\rho_{g}}{\bar{\alpha}_{g}}\bar{u}_{g}\right] 
+ \left[\frac{\partial^{2}h'_{i}}{\partial z^{2}}\right]\left[\frac{\rho_{l}}{\bar{\alpha}_{l}}\bar{u}_{l}^{2} + \frac{\rho_{g}}{\bar{\alpha}_{g}}\bar{u}_{g}^{2} - (\rho_{l} - \rho_{g})g\frac{dh_{i}}{d\alpha_{l}} - \left(\rho_{l}\frac{\partial h'_{g,l}}{\partial \alpha_{l}} - \rho_{g}\frac{\partial h'_{g,g}}{\partial \alpha_{l}}\right)g\right] + \left[\frac{\partial^{4}h'_{i}}{\partial z^{4}}\right]\left[\frac{dh_{i}}{d\alpha_{l}}\sigma\right] 
+ \left[\frac{\partial h'_{i}}{\partial t}\right]\left[\frac{\partial F}{\partial u_{g}}\frac{1}{\alpha_{g}} - \frac{\partial F}{\partial u_{l}}\frac{1}{\alpha_{l}}\right] + \left[\frac{\partial h'_{i}}{\partial z}\right]\left[\frac{\partial F}{\partial u_{g}}\frac{\bar{u}_{g}}{\alpha_{g}} - \frac{\partial F}{\partial u_{l}}\frac{\bar{u}_{l}}{\alpha_{l}} + \frac{\partial F}{\partial \alpha_{l}}\right] = 0$$
(13)

The considerations on the sine shape of the perturbation lead to the following expression for the perturbed liquid level:

$$h_i' = \epsilon \exp^{i(\omega t - kz)} \tag{14}$$

This results in a quadratic equation (Equ.15) for the wave frequency, called the dispersion equation:

$$\omega^2 - 2\left(\mathbf{a}\,k - \mathbf{b}\,i\right)\omega + \mathbf{c}\,k^2 - \mathbf{d}\,k^4 - \mathbf{e}\,k\,i = 0 \tag{15}$$

where:

$$\rho_{tot} = \left[ \frac{\rho_l}{\bar{\alpha}_l} + \frac{\rho_g}{\bar{\alpha}_g} \right] 
\mathbf{a} = \frac{1}{\rho_{tot}} \left[ \frac{\rho_l}{\bar{\alpha}_l} \bar{u}_l + \frac{\rho_g}{\bar{\alpha}_g} \bar{u}_g \right] 
\mathbf{b} = -\frac{1}{\rho_{tot}} \frac{1}{2} \left[ \frac{\partial F}{\partial u_g} \frac{1}{\alpha_g} - \frac{\partial F}{\partial u_l} \frac{1}{\alpha_l} \right] 
\mathbf{c} = \frac{1}{\rho_{tot}} \left[ \frac{\rho_l}{\bar{\alpha}_l} \bar{u}_l^2 + \frac{\rho_g}{\bar{\alpha}_g} \bar{u}_g^2 - (\rho_l - \rho_g) g \frac{dh_i}{d\alpha_l} - \left( \rho_l \frac{\partial h_{g,l}^-}{\partial \alpha_l} - \rho_g \frac{\partial h_{g,g}^-}{\partial \alpha_l} \right) g \right] 
\mathbf{d} = \frac{1}{\rho_{tot}} \left[ \frac{dh_i}{d\alpha_l} \sigma \right] 
\mathbf{e} = -\frac{1}{\rho_{tot}} \left[ \frac{\partial F}{\partial u_g} \frac{\bar{u}_g}{\alpha_g} - \frac{\partial F}{\partial u_l} \frac{\bar{u}_l}{\alpha_l} + \frac{\partial F}{\partial \alpha_l} \right]$$
(16)

The solutions for  $\omega$  are:

$$\omega_{1} = (\mathbf{a} k - \mathbf{b} i) + \sqrt[4]{\beta^{2} + \gamma^{2}} \exp i \frac{1}{2} \arctan \left(\frac{\gamma}{\beta}\right)$$

$$\omega_{2} = (\mathbf{a} k - \mathbf{b} i) + \sqrt[4]{\beta^{2} + \gamma^{2}} \exp i \frac{1}{2} \left[\arctan \left(\frac{\gamma}{\beta}\right) + 2\pi\right]$$
(17)

with the coefficients:

$$\beta = (\mathbf{a}^2 - \mathbf{c}) k^2 + \mathbf{d} k^4 - \mathbf{b}^2$$

$$\gamma = \mathbf{e} k - 2 \mathbf{a} \mathbf{b} k$$
(18)

Thus the linear stability analysis provides a relation between the angular frequency  $\omega$  and the wave number k. By decoupling the angular frequency in a real and an imaginary parts, the perturbation (Equ. 14) becomes:

$$h_i' = \epsilon \exp^{i((\omega_R + i\omega_I)t - kz)} = \epsilon \exp^{i(\omega_R t - kz)} \exp^{-\omega_I t}$$
(19)

The first exponential in Equ. 19 corresponds to a solution of a wave equation. The second term drives the amplification because for all conditions which make this term higher than one, the waves will growth with time. Consequently the steady-state solution is unstable whenever the imaginary part of  $\omega$  is negative.

## 3.1 Closure laws

The viscous approach for determining the most amplified wavelength for a given set of conditions requires closure laws for wall and interfacial shear stresses. The shear stresses modeling is a key parameter of the stability study because the outcome of the analysis depends heavily on its modeling. The results presented here are obtained based on the classical laws from Taitel and Dukler [12] and slightly corrected by Barnea and Taitel [11]:

$$\tau_{w,k} = \frac{1}{2} f_k \rho_k u_k |u_k| \tag{20}$$

$$\tau_i = \frac{1}{2} f_i \rho_g (u_g - u_l) |u_g - u_l|$$
 (21)

where the friction coefficient is (with a  $Re_k = \frac{\rho_k |u_k| D_k}{u_k}$ ):

$$f_k = C_k Re_k^{-n_k}$$

if  $Re_k > 2000 \Rightarrow C_k = 0.046 \quad n_k = 0.2$ 

else  $Re_k < 2000 \Rightarrow C_k = 16 \quad n_k = 1$ 

(22)

if  $f_g > 0.0142 \quad f_i = f_g$ 

else  $f_g < 0.0142 \quad f_i = 0.0142$ 

# 4 Some results of the stability analysis

The initial void fraction is matched to each case according to the two superficial velocities, at its steady and established flow value, obtained after combining Equ. 9 assuming  $\frac{\partial \alpha}{\partial z} = 0$  and  $\frac{\partial \alpha}{\partial t} = 0$ .

$$\alpha_g = \frac{\xi_i \, \tau_i + \xi_g \, \tau_g}{\xi_l \, \tau_l + \xi_g \, \tau_g} \tag{23}$$

where  $\xi_i$  is the curvilinear length of the interface,  $\xi_l$  and  $\xi_g$  the wetted perimeter and the dry perimeter in the cross-section plane. he plots on Fig. 2 show results of the linear stability analysis in two particular cases. The evolution of the amplification rate for all possible wavelengths of pipe equivalent diameters of  $D_h = 0.1 \, m$  (Fig. 2a) and  $D_h = 0.24 \, m$  (Fig. 2b) and the flow conditions of the REGARD experiments which will be devoted to the validation of the entrainment model. It may be important to mention that available experimental results on wave formation or entrainment phenomenon in the literature cover rather small diameters up to  $0.095 \, m$  [3]. These curves show a peak of amplification factor at the most amplified wavelength; this latter value is the interesting parameter for the entrainment model as the amplification factor acts only in the time development of the perturbation  $h_i'$  of unknown initial amplitude  $\epsilon$ .

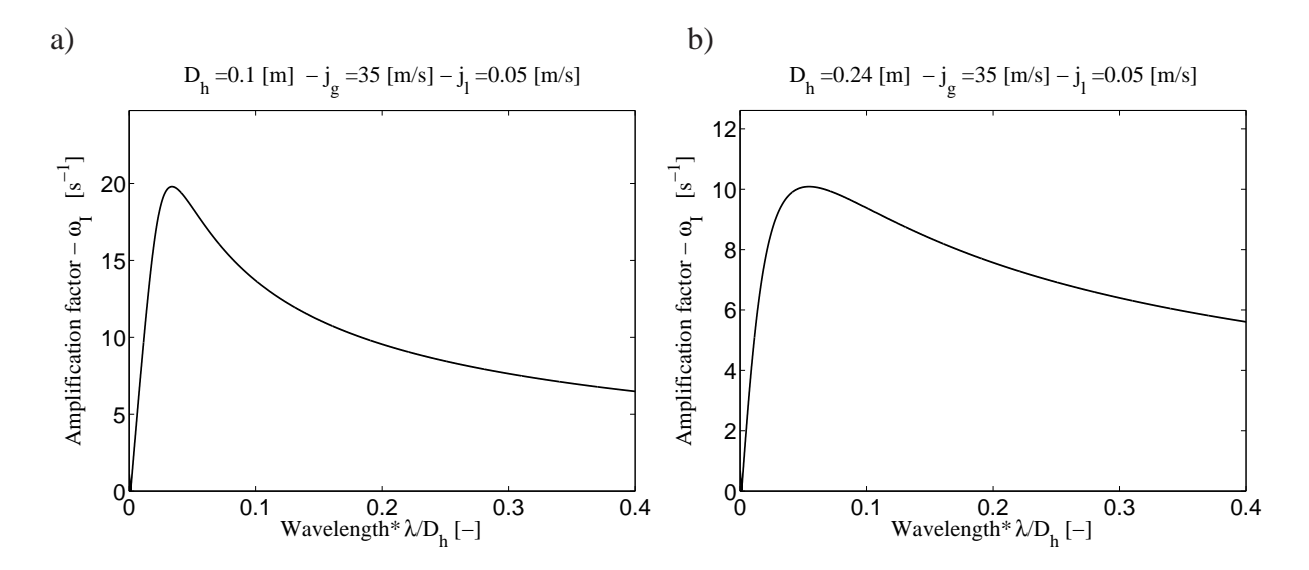


Figure 2: Amplification rate for all wavelength for given sets of fluid characteristics and comparison between the proposed model and the results of Barnea and Taitel

The flow characteristics used for these calculations are  $\rho_l = 940 \left[\frac{kg}{m^3}\right]$ ,  $\rho_g = 1 \left[\frac{kg}{m^3}\right]$ ,  $\mu_l = 7.97 \, 10^{-4} \left[\frac{kg}{ms}\right]$ ,  $\mu_g = 1.2 \, 10^{-5} \left[\frac{kg}{ms}\right]$ , and  $\sigma = 0.07 \left[\frac{kg}{s^2}\right]$ . The critical wave number and the range of wave numbers being most amplified depend on the flow conditions as shown on the different plots of Fig. 3. It is observed that the range of most amplified waves is broadened when the liquid superficial velocity is decreased for a given gas superficial velocity and pipe diameter, while the amplification factors are strongly decreased. Increasing the gas superficial velocity in the same conditions has a similar effect.

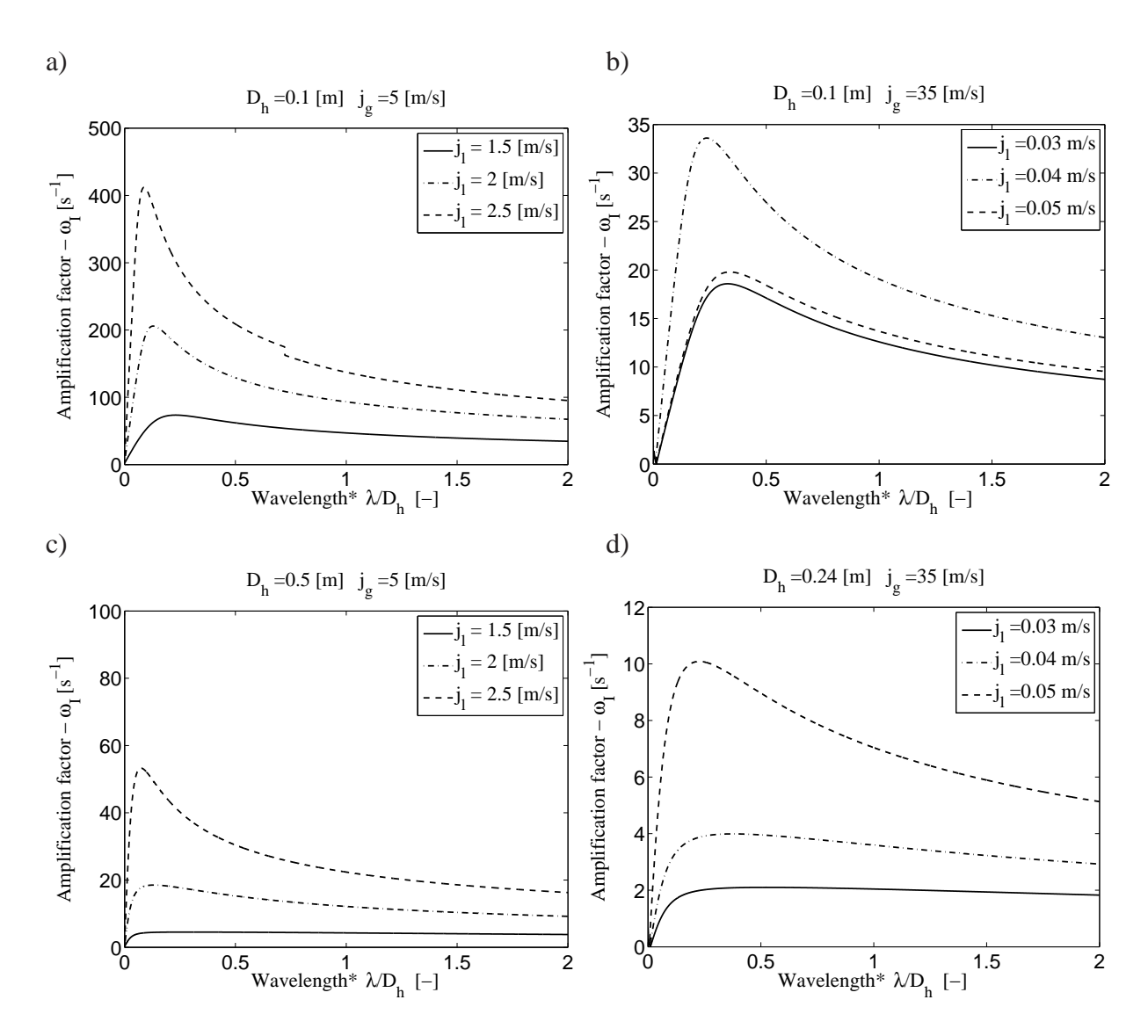


Figure 3: Effects of  $j_l$  on the critical wavelength for pipe diameters of 0.01 m, 0.24 m and 0.50 m and gas superficial velocities of 5  $m.s^{-1}$ , 10  $m.s^{-1}$  and 35  $m.s^{-1}$ 

The influence of the pipe diameter is not significant on the value of the most amplified wave number and its bandwidth, except for the largest gas superficial velocity (Figs. 3b-d) or at low liquid velocities, where a decrease of pipe diameter involves a more pronounced broadening of the range of amplified wave numbers. Furthermore, increasing the pipe diameter always strongly decreases the amplification factors. These results illustrate the need for new experiments at large diameters, closer to those of full scale situations contrary to what is available in the literature.

# 4.1 A correlation for the critical wavelength

In the case of a full computation of a LOCA situation with CATHARE, the mesh resolution for the hot leg pipe could be fairly low such as a control volume could include several ripples. Therefore, it could be necessary to run the stability analysis in each cell and at each timestep, which would be very time-consuming. In regards to this issue, a correlation based on the previous stability analysis has been set up in order to evaluate the critical wavelength as a function of the flow and geometry (equivalent diameter) conditions.

A multiple non-linear regression is performed on a large set of results to make a correlation providing a maximum difference of 5% compared to the results obtained with the full linear stability analysis. The range of validity of this correlation is  $[0.1 < D_h < 0.5]$  for stratified horizontal flows with liquid and gas superficial velocities indicated on Fig. 4. The proposed

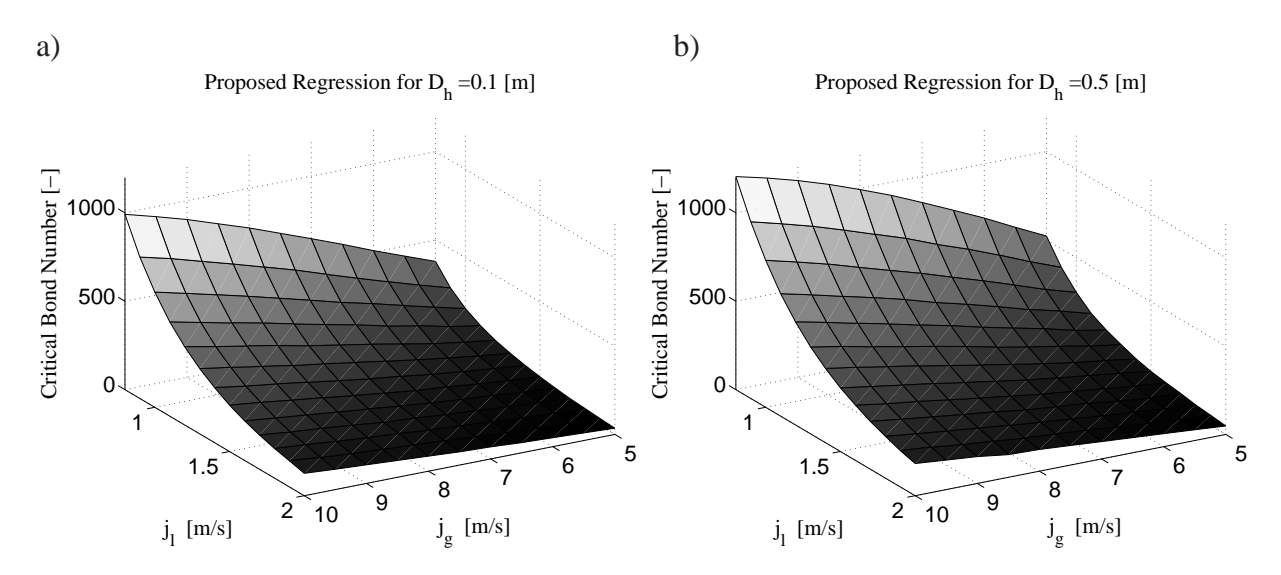


Figure 4: Predictions of the proposed correlation

correlation (Equ. 24) is cast in terms of a critical Eötvös ( $Eo^*$ ) or Bond ( $Bo^*$ ) number where the characteristics length is the critical wavelength:

$$\sqrt{Bo^*} = 0.078 \,\alpha_l^{1.7083} \,\alpha_g^{1.0109} \,Re_l^{1.041} \,Re_g^{0.1747} \,Fr^{0.0088} \,D_h^{-1.1382} \tag{24}$$

with

$$Bo = Eo = \frac{L_{carac}^2}{L_{Laplace}^2} \tag{25}$$

$$L_{\text{Laplace}} = \sqrt{\frac{\sigma}{\Delta \rho \, q}} = 0.0028 \, m \tag{26}$$

# 5 Evaluation of the entrained volume

Here a mechanistic approach based on a force balance is preferred to obtain a model for the entrained volume as it was proposed for vertical annular flow by Holowach et al. [6]. The wave fragmentation is assumed to occur when the resultant of forces acting on a ripple wave crest changes from vertical downward to upward direction, e.g. passing through the equilibrium situation. The forces included in the model are the gravity, the surface tension, the drag and

the lift forces. Compared to a similar study [6] conducted in vertical flow conditions, a lift and a gravity forces are added, and the components of those forces have different orientations. Consequently, the proposed model is only valid for stratified flows in horizontal pipes. The force balance when the conditions are fulfilled to pull-up a certain part of the wave into droplets is then:

$$F_{d,y} + F_{l,y} + F_{g,y} + F_{\sigma,y} = 0 (27)$$

where the different forces are detailed below (Equ. 28, Equ. 30, Equ. 32). The lift/drag forces (Equ. 28) are calculated by giving a lift/drag coefficient  $C_L/C_D$ , using the relative velocity of the ripple wave crest  $(v_{cr})$ , and by estimating the effective (entrained) area (Fig. 5) on which the drag and the lift forces act:

$$F_{l,y} = 0.5 \,\rho_g \,C_L \,A_{entr} \,\left(v_g - v_{cr}\right)^2 \tag{28}$$

where many correlations could be used for evaluating  $C_L/C_D$ , for instance the correlation used in [6]. As the wave is assumed to have a three-dimensional sine topology, the surface integration gives:

$$A_{entr}(h,b,\lambda) = \frac{h\lambda}{\pi}\cos\left(\frac{2\pi b}{\lambda}\right) - \left(\frac{h\lambda}{2} - 2hb\right)\sin\left(\frac{2\pi b}{\lambda}\right)$$
(29)

The gravitational force is expressed as:

$$F_{q,y} = -\rho_l V_{entr} g \tag{30}$$

where the entrained volume on which the gravitational force acts is defined by using the disc integration method:

$$V_{entr}(h,b,\lambda) = \pi \left(\frac{\lambda}{4} - b\right) \frac{h^2 \left(\frac{\lambda}{2} - b\right)^2 - \sin\left(\frac{2\pi b}{\lambda}\right) \frac{\lambda^2}{16}}{\left(\frac{\lambda}{2} - b\right)^2 - \frac{\lambda^2}{16}} - \pi \frac{h^2 - \sin^2\left(\frac{2\pi b}{\lambda}\right)}{3\left(\frac{\lambda}{2} - b\right)^2 - \frac{\lambda^2}{16}} \left(\left(\frac{\lambda}{2} - b\right)^3 - \left(\frac{\lambda}{4}\right)^3\right)$$
(31)

Finally the surface tension force is expressed as:

$$F_{\sigma,y} = -\sigma K_{crest} A_{\sigma} \tag{32}$$

where  $K_{crest}$  is the average curvature at the crest area and  $A_{\sigma}$  is the effective area on which the surface tension acts. These two geometric parameters are expressed as follows:

$$A_{\sigma}(b,\lambda) = \pi \left(\frac{\frac{\lambda}{4} - b}{2}\right)^2 \tag{33}$$

$$K_{crest}(h) = \frac{4\pi^2 h}{\lambda^2} \tag{34}$$

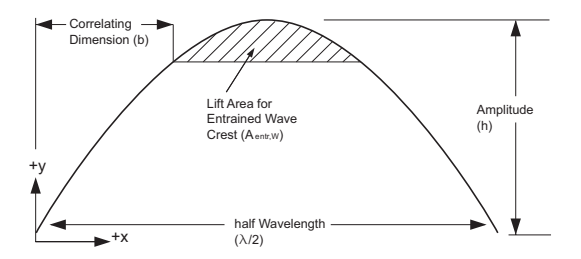


Figure 5: Main geometric parameters describing a ripple

The geometric parameters of these forces are expressed as functions of three critical parameters: h the amplitude of the wave at the onset of fragmentation, b a geometrical parameter corresponding to the horizontal distance between the base of the wave and the location of the fragmentation, and  $\lambda$  the wavelength of the ripple. Therefore the sum of the various forces exerted on the crest of the wave is a function of those three simple parameters. By knowing the amplitude h at the onset of fragmentation, the entrained volume is found out by simple iterations on the size b until the force balance is checked. This assumes to know the evolution of the amplification factor up to the onset of the entrainment phenomenon.

#### 6 Conclusion

In this paper, an extension of the model proposed by Holowach et al. [6] to the case of horizontal wavy stratified flows has been presented. The mechanistic approach requires several level of modeling and assumptions. Even though some important parameters such as the entrainment time scale and the criterion to determine the amplitude of the waves at the onset of their fragmentation require further investigations, it was shown that a relatively simple methodology could be established to evaluate the source term to add in the dispersed phase conservation equation. Once the complete model achieved, the next step will be to compare the results to new experimental data performed at a large pipe diameter (about  $0.24\,m$ ). This experiment, called REGARD is under development at CEA Grenoble, France. This analysis will allow to improve the model in order to obtain averaged entrainment rates matching with this experiment. It is believed that the results will be more suited for simulations of droplet entrainment in a full scale hot leg.

# Akwnoldgements

The present work has been performed as part of the EDF-CEA Neptune project, with the financial support of AREVA-NP and IRSN.

#### References

- [1] P. Hutchinson and P. B. Whalley. A possible characterisation of entrainment in annular flow. *Chemical Engineering Science*, 28:974–975, 1973.
- [2] G. F. Hewitt and A. H. Govan. Phenomenological modelling of non-equilibrium flows with phase change. *Int. J. Heat Mass Transfer*, 33:229–242, 1990.
- [3] L. R. Williams, L. A. Dykhno, and T. J. Hanratty. Droplet flux distributions and entrainment in horizontal gas-liquid flows. *Int. J. Multiphase Flow*, 22:1–18, 1996.
- [4] S. A. Schadel, G. W. Leman, G. W. Binder, and T. J. Hanratty. Rates of atomization and deposition in vertical annular flow. *Int. J. Multiphase Flow*, 16:363–374, 1990.
- [5] D. F. Woodmansee and T. J. Hanratty. Mechanism for the removal of droplets from a liquid surface by a parallel air flow. *Chemical Engineering Science*, 24:299–307, 1969.
- [6] M. J. Holowach, I. E. Hochreiter, and F. B. Cheung. A model for droplet entrainment in heated annular flow. *Int. J. Heat and Fluid Flow*, 23:807–822, 2002.

- [7] F. de Crecy. Etude des écoulements stratifiés dans une conduite. CEA Grenoble, 1981.
- [8] D. Barnea and Y. Taitel. Kelvin-helmholtz stability criteria for stratified flow: viscous versus non viscous (inviscid) approaches. *Int. J. Multiphase Flow*, 19:639–649, 1993.
- [9] P. Y. Lin and T. J. Hanratty. Prediction of initiation of slugs with linear stability theory. *Int. J. Multiphase Flow*, 12:79–98, 1986.
- [10] P. Y. Lin and T. J. Hanratty. Effect of pipe diameter on the interfacial configurations for air-water flow in horizontal pipes. *Int. J. Multiphase Flow*, 13:549–563, 1987.
- [11] D. Barnea and Y. Taitel. Transient-formulation modes and stability of steady-state annular flow. *Chemical Engineering Science*, 44:325–332, 1989.
- [12] Y. Taitel and A. E. Dukler. A model for prediction of flow regime transitions in horizontal and near horizontal gas-liquid flow. *AIChE J.*, 22:47–55, 1976.